

Search for anomalous production of diphoton events with missing transverse energy at CDF and limits on gauge-mediated supersymmetry-breaking models

CDF Collaboration

CAMPANELLI, Mario (Collab.), *et al.*

Abstract

We present the results of a search for anomalous production of diphoton events with large missing transverse energy using the Collider Detector at Fermilab. In 202 pb^{-1} of pp collisions at $s\sqrt{=}1.96 \text{ TeV}$ we observe no candidate events, with an expected standard model background of $0.27 \pm 0.07(\text{stat}) \pm 0.10(\text{syst})$ events. The results exclude a lightest chargino of mass less than $167 \text{ GeV}/c^2$, and lightest neutralino of mass less than $93 \text{ GeV}/c^2$ at 95% C.L. in a gauge-mediated supersymmetry-breaking model with a light gravitino.

CDF Collaboration, CAMPANELLI, Mario (Collab.), *et al.* Search for anomalous production of diphoton events with missing transverse energy at CDF and limits on gauge-mediated supersymmetry-breaking models. *Physical Review. D*, 2005, vol. 71, no. 03, p. 031104

DOI : 10.1103/PhysRevD.71.031104

Available at:

<http://archive-ouverte.unige.ch/unige:38286>

Disclaimer: layout of this document may differ from the published version.



Search for anomalous production of diphoton events with missing transverse energy at CDF and limits on gauge-mediated supersymmetry-breaking models

D. Acosta,¹⁶ J. Adelman,¹² T. Affolder,⁹ T. Akimoto,⁵⁴ M. G. Albrow,¹⁵ D. Ambrose,⁴³ S. Amerio,⁴² D. Amidei,³³ A. Anastassov,⁵⁰ K. Anikeev,³¹ A. Annovi,⁴⁴ J. Antos,¹ M. Aoki,⁵⁴ G. Apollinari,¹⁵ T. Arisawa,⁵⁶ J-F. Arguin,³² A. Artikov,¹³ W. Ashmanskas,¹⁵ A. Attal,⁷ F. Azfar,⁴¹ P. Azzi-Bacchetta,⁴² N. Bacchetta,⁴² H. Bachacou,²⁸ W. Badgett,¹⁵ A. Barbaro-Galtieri,²⁸ G. J. Barker,²⁵ V. E. Barnes,⁴⁶ B. A. Barnett,²⁴ S. Baroiant,⁶ M. Barone,¹⁷ G. Bauer,³¹ F. Bedeschi,⁴⁴ S. Behari,²⁴ S. Belforte,⁵³ G. Bellettini,⁴⁴ J. Bellinger,⁵⁸ E. Ben-Haim,¹⁵ D. Benjamin,¹⁴ A. Beretvas,¹⁵ A. Bhatti,⁴⁸ M. Binkley,¹⁵ D. Bisello,⁴² M. Bishai,¹⁵ R. E. Blair,² C. Blocker,⁵ K. Bloom,³³ B. Blumenfeld,²⁴ A. Bocci,⁴⁸ A. Bodek,⁴⁷ G. Bolla,⁴⁶ A. Bolshov,³¹ P. S. L. Booth,²⁹ D. Bortoletto,⁴⁶ J. Boudreau,⁴⁵ S. Bourov,¹⁵ C. Bromberg,³⁴ E. Brubaker,¹² J. Budagov,¹³ H. S. Budd,⁴⁷ K. Burkett,¹⁵ G. Busetto,⁴² P. Bussey,¹⁹ K. L. Byrum,² S. Cabrera,¹⁴ M. Campanelli,¹⁸ M. Campbell,³³ A. Canepa,⁴⁶ M. Casarsa,⁵³ D. Carlsmith,⁵⁸ S. Carron,¹⁴ R. Carosi,⁴⁴ M. Cavalli-Sforza,³ A. Castro,⁴ P. Catastini,⁴⁴ D. Cauz,⁵³ A. Cerri,²⁸ L. Cerrito,²³ J. Chapman,³³ C. Chen,⁴³ Y. C. Chen,¹ M. Chertok,⁶ G. Chiarelli,⁴⁴ G. Chlachidze,¹³ F. Chlebana,¹⁵ I. Cho,²⁷ K. Cho,²⁷ D. Chokheli,¹³ J. P. Chou,²⁰ M. L. Chu,¹ S. Chuang,⁵⁸ J. Y. Chung,³⁸ W-H. Chung,⁵⁸ Y. S. Chung,⁴⁷ C. I. Ciobanu,²³ M. A. Ciocci,⁴⁴ A. G. Clark,¹⁸ D. Clark,⁵ M. Coca,⁴⁷ A. Connolly,²⁸ M. Convery,⁴⁸ J. Conway,⁶ B. Cooper,³⁰ M. Cordelli,¹⁷ G. Cortiana,⁴² J. Cranshaw,⁵² J. Cuevas,¹⁰ R. Culbertson,¹⁵ C. Currat,²⁸ D. Cyr,⁵⁸ D. Dagenhart,⁵ S. Da Ronco,⁴² S. D'Auria,¹⁹ P. de Barbaro,⁴⁷ S. De Cecco,⁴⁹ G. De Lentdecker,⁴⁷ S. Dell'Agnello,¹⁷ M. Dell'Orso,⁴⁴ S. Demers,⁴⁷ L. Demortier,⁴⁸ M. Deninno,⁴ D. De Pedis,⁴⁹ P. F. Derwent,¹⁵ C. Dionisi,⁴⁹ J. R. Dittmann,¹⁵ P. Doksus,²³ A. Dominguez,²⁸ S. Donati,⁴⁴ M. Donega,¹⁸ J. Donini,⁴² M. D'Onofrio,¹⁸ T. Dorigo,⁴² V. Drollinger,³⁶ K. Ebina,⁵⁶ N. Eddy,²³ R. Ely,²⁸ R. Erbacher,⁶ M. Erdmann,²⁵ D. Errede,²³ S. Errede,²³ R. Eusebi,⁴⁷ H-C. Fang,²⁸ S. Farrington,²⁹ I. Fedorko,⁴⁴ W. T. Fedorko,¹² R. G. Feild,⁵⁹ M. Feindt,²⁵ J. P. Fernandez,⁴⁶ C. Ferretti,³³ R. D. Field,¹⁶ G. Flanagan,³⁴ B. Flaugher,¹⁵ L. R. Flores-Castillo,⁴⁵ A. Foland,²⁰ S. Forrester,⁶ G. W. Foster,¹⁵ M. Franklin,²⁰ J. C. Freeman,²⁸ H. Frisch,¹² Y. Fujii,²⁶ I. Furic,¹² A. Gajjar,²⁹ A. Gallas,³⁷ J. Galyardt,¹¹ M. Gallinaro,⁴⁸ A. F. Garfinkel,⁴⁶ C. Gay,⁵⁹ H. Gerberich,¹⁴ D. W. Gerdes,³³ E. Gerchtein,¹¹ S. Giagu,⁴⁹ P. Giannetti,⁴⁴ A. Gibson,²⁸ K. Gibson,¹¹ C. Ginsburg,⁵⁸ K. Giolo,⁴⁶ M. Giordani,⁵³ M. Giunta,⁴⁴ G. Giurgiu,¹¹ V. Glagolev,¹³ D. Glenzinski,¹⁵ M. Gold,³⁶ N. Goldschmidt,³³ D. Goldstein,⁷ J. Goldstein,⁴¹ G. Gomez,¹⁰ G. Gomez-Ceballos,³¹ M. Goncharov,⁵¹ O. González,⁴⁶ I. Gorelov,³⁶ A. T. Goshaw,¹⁴ Y. Gotra,⁴⁵ K. Goulianos,⁴⁸ A. Gresele,⁴ M. Griffiths,²⁹ C. Grosso-Pilcher,⁴⁷ U. Grundler,²³ M. Guenther,⁴⁶ J. Guimaraes da Costa,²⁰ C. Haber,²⁸ K. Hahn,⁴³ S. R. Hahn,¹⁵ E. Halkiadakis,⁴⁷ A. Hamilton,³² B-Y. Han,⁴⁷ R. Handler,⁵⁸ F. Happacher,¹⁷ K. Hara,⁵⁴ M. Hare,⁵⁵ R. F. Harr,⁵⁷ R. M. Harris,¹⁵ F. Hartmann,²⁵ K. Hatakeyama,⁴⁸ J. Hauser,⁷ C. Hays,¹⁴ H. Hayward,²⁹ E. Heider,⁵⁵ B. Heinemann,²⁹ J. Heinrich,⁴³ M. Hennecke,²⁵ M. Herndon,²⁴ C. Hill,⁹ D. Hirschbuehl,²⁵ A. Hocker,⁴⁷ K. D. Hoffman,¹² A. Holloway,²⁰ S. Hou,¹ M. A. Houlden,²⁹ B. T. Huffman,⁴¹ Y. Huang,¹⁴ R. E. Hughes,³⁸ J. Huston,³⁴ K. Ikado,⁵⁶ J. Incandela,⁹ G. Introzzi,⁴⁴ M. Iori,⁴⁹ Y. Ishizawa,⁵⁴ C. Issever,⁹ A. Ivanov,⁴⁷ Y. Iwata,²² B. Iyutin,³¹ E. James,¹⁵ D. Jang,⁵⁰ J. Jarrell,³⁶ D. Jeans,⁴⁹ H. Jensen,¹⁵ E. J. Jeon,²⁷ M. Jones,⁴⁶ K. K. Joo,²⁷ S. Jun,¹¹ T. Junk,²³ T. Kamon,⁵¹ J. Kang,³³ M. Karagoz Unel,³⁷ P. E. Karchin,⁵⁷ S. Kartal,¹⁵ Y. Kato,⁴⁰ Y. Kemp,²⁵ R. Kephart,¹⁵ U. Kerzel,²⁵ V. Khotilovich,⁵¹ B. Kilminster,³⁸ D. H. Kim,²⁷ H. S. Kim,²³ J. E. Kim,²⁷ M. J. Kim,¹¹ M. S. Kim,²⁷ S. B. Kim,²⁷ S. H. Kim,⁵⁴ T. H. Kim,³¹ Y. K. Kim,¹² B. T. King,²⁹ M. Kirby,¹⁴ L. Kirsch,⁵ S. Klimenko,¹⁶ B. Knuteson,³¹ B. R. Ko,¹⁴ H. Kobayashi,⁵⁴ P. Koehn,³⁸ D. J. Kong,²⁷ K. Kondo,⁵⁶ J. Konigsberg,¹⁶ K. Kordas,³² A. Korn,³¹ A. Korytov,¹⁶ K. Kotelnikov,³⁵ A. V. Kotwal,¹⁴ A. Kovalev,⁴³ J. Kraus,²³ I. Kravchenko,³¹ A. Kreymer,¹⁵ J. Kroll,⁴³ M. Kruse,¹⁴ V. Krutelyov,⁵¹ S. E. Kuhlmann,² N. Kuznetsova,¹⁵ A. T. Laasanen,⁴⁶ S. Lai,³² S. Lami,⁴⁸ S. Lammel,¹⁵ J. Lancaster,¹⁴ M. Lancaster,³⁰ R. Lander,⁶ K. Lannon,³⁸ A. Lath,⁵⁰ G. Latino,³⁶ R. Lauhakangas,²¹ I. Lazzizzera,⁴² Y. Le,²⁴ C. Lecci,²⁵ T. LeCompte,² J. Lee,²⁷ J. Lee,⁴⁷ S. W. Lee,⁵¹ R. Lefèvre,³ N. Leonardo,³¹ S. Leone,⁴⁴ J. D. Lewis,¹⁵ K. Li,⁵⁹ C. Lin,⁵⁹ C. S. Lin,¹⁵ M. Lindgren,¹⁵ T. M. Liss,²³ D. O. Litvintsev,¹⁵ T. Liu,¹⁵ Y. Liu,¹⁸ N. S. Lockyer,⁴³ A. Loginov,³⁵ M. Loreti,⁴² P. Loverre,⁴⁹ R-S. Lu,¹ D. Lucchesi,⁴² P. Lujan,²⁸ P. Lukens,¹⁵ G. Lungu,¹⁶ L. Lyons,⁴¹ J. Lys,²⁸ R. Lysak,¹ D. MacQueen,³² R. Madrak,²⁰ K. Maeshima,¹⁵ P. Maksimovic,²⁴ L. Malferrari,⁴ G. Manca,²⁹ R. Marginean,³⁸ M. Martin,²⁴ A. Martin,⁵⁹ V. Martin,³⁷ M. Martínez,³ T. Maruyama,⁵⁴ H. Matsunaga,⁵⁴ M. Mattson,⁵⁷ P. Mazzanti,⁴ K. S. McFarland,⁴⁷ D. McGivern,³⁰ P. M. McIntyre,⁵¹ P. McNamara,⁵⁰ R. McNulty,²⁹ S. Menzemer,³¹ A. Menzione,⁴⁴ P. Merkel,¹⁵ C. Mesropian,⁴⁸ A. Messina,⁴⁹ T. Miao,¹⁵ N. Miladinovic,⁵ L. Miller,²⁰ R. Miller,³⁴ J. S. Miller,³³ R. Miquel,²⁸ S. Miscetti,¹⁷ G. Mitselmakher,¹⁶ A. Miyamoto,²⁶ Y. Miyazaki,⁴⁰ N. Moggi,⁴ B. Mohr,⁷ R. Moore,¹⁵ M. Morello,⁴⁴ A. Mukherjee,¹⁵ M. Mulhearn,³¹ T. Muller,²⁵ R. Mumford,²⁴ A. Munar,⁴³ P. Murat,¹⁵ J. Nachtman,¹⁵ S. Nahn,⁵⁹ I. Nakamura,⁴³ I. Nakano,³⁹ A. Napier,⁵⁵ R. Napora,²⁴ D. Naumov,³⁶ V. Necula,¹⁶ F. Niell,³³ J. Nielsen,²⁸ C. Nelson,¹⁵ T. Nelson,¹⁵ C. Neu,⁴³ M. S. Neubauer,⁸

C. Newman-Holmes,¹⁵ A-S. Nicollerat,¹⁸ T. Nigmanov,⁴⁵ L. Nodulman,² O. Norriella,³ K. Oesterberg,²¹ T. Ogawa,⁵⁶ S. H. Oh,¹⁴ Y. D. Oh,²⁷ T. Ohsugi,²² T. Okusawa,⁴⁰ R. Oldeman,⁴⁹ R. Orava,²¹ W. Orejudos,²⁸ C. Pagliarone,⁴⁴ E. Palencia,¹⁰ R. Paoletti,⁴⁴ V. Papadimitriou,¹⁵ S. Pashapour,³² J. Patrick,¹⁵ G. Pauletta,⁵³ M. Paulini,¹¹ T. Pauly,⁴¹ C. Paus,³¹ D. Pellett,⁶ A. Penzo,⁵³ T. J. Phillips,¹⁴ G. Piacentino,⁴⁴ J. Piedra,¹⁰ K. T. Pitts,²³ C. Plager,⁷ A. Pompoš,⁴⁶ L. Pondrom,⁵⁸ G. Pope,⁴⁵ O. Poukhov,¹³ F. Prakoshyn,¹³ T. Pratt,²⁹ A. Pronko,¹⁶ J. Proudfoot,² F. Ptohos,¹⁷ G. Punzi,⁴⁴ J. Rademacker,⁴¹ A. Rakitine,³¹ S. Rappoccio,²⁰ F. Ratnikov,⁵⁰ H. Ray,³³ A. Reichold,⁴¹ B. Reiser,¹⁵ V. Rekovic,³⁶ P. Renton,⁴¹ M. Rescigno,⁴⁹ F. Rimondi,⁴ K. Rinnert,²⁵ L. Ristori,⁴⁴ W. J. Robertson,¹⁴ A. Robson,⁴¹ T. Rodrigo,¹⁰ S. Rolli,⁵⁵ L. Rosenson,³¹ R. Roser,¹⁵ R. Rossin,⁴² C. Rott,⁴⁶ J. Russ,¹¹ V. Rusu,¹² A. Ruiz,¹⁰ D. Ryan,⁵⁵ H. Saarikko,²¹ S. Sabik,³² A. Safonov,⁶ R. St. Denis,¹⁹ W. K. Sakumoto,⁴⁷ G. Salamanna,⁴⁹ D. Saltzberg,⁷ C. Sanchez,³ A. Sansoni,¹⁷ L. Santi,⁵³ S. Sarkar,⁴⁹ K. Sato,⁵⁴ P. Savard,³² A. Savoy-Navarro,¹⁵ P. Schlabach,¹⁵ E. E. Schmidt,¹⁵ M. P. Schmidt,⁵⁹ M. Schmitt,³⁷ L. Scodellaro,⁴² A. Scribano,⁴⁴ F. Scuri,⁴⁴ A. Sedov,⁴⁶ S. Seidel,³⁶ Y. Seiya,⁴⁰ F. Semeria,⁴ L. Sexton-Kennedy,¹⁵ I. Sfiligoi,¹⁷ M. D. Shapiro,²⁸ T. Shears,²⁹ P. F. Shepard,⁴⁵ D. Sherman,²⁰ M. Shimojima,⁵⁴ M. Shochet,¹² Y. Shon,⁵⁸ I. Shreyber,³⁵ A. Sidoti,⁴⁴ J. Siegrist,²⁸ M. Siket,¹ A. Sill,⁵² P. Sinervo,³² A. Sisakyan,¹³ A. Skiba,²⁵ A. J. Slaughter,¹⁵ K. Sliwa,⁵⁵ D. Smirnov,³⁶ J. R. Smith,⁶ F. D. Snider,¹⁵ R. Snihur,³² A. Soha,⁶ S. V. Somalwar,⁵⁰ J. Spalding,¹⁵ M. Spezziga,⁵² L. Spiegel,¹⁵ F. Spinella,⁴⁴ M. Spiropulu,⁹ P. Squillacioti,⁴⁴ H. Stadie,²⁵ B. Stelzer,³² O. Stelzer-Chilton,³² J. Strologas,³⁶ D. Stuart,⁹ A. Sukhanov,¹⁶ K. Sumorok,³¹ H. Sun,⁵⁵ T. Suzuki,⁵⁴ A. Taffard,²³ R. Tafirout,³² S. F. Takach,⁵⁷ H. Takano,⁵⁴ R. Takashima,²² Y. Takeuchi,⁵⁴ K. Takikawa,⁵⁴ M. Tanaka,² R. Tanaka,³⁹ N. Tanimoto,³⁹ S. Tapprogge,²¹ M. Tecchio,³³ P. K. Teng,¹ K. Terashi,⁴⁸ R. J. Tesarek,¹⁵ S. Tether,³¹ J. Thom,¹⁵ A. S. Thompson,¹⁹ E. Thomson,⁴³ P. Tipton,⁴⁷ V. Tiwari,¹¹ S. Tkaczyk,¹⁵ D. Toback,⁵¹ K. Tollefson,³⁴ T. Tomura,⁵⁴ D. Tonelli,⁴⁴ M. Tönnemann,³⁴ S. Torre,⁴⁴ D. Torretta,¹⁵ S. Tourneur,¹⁵ W. Trischuk,³² J. Tseng,⁴¹ R. Tsuchiya,⁵⁶ S. Tsuno,³⁹ D. Tsybychev,¹⁶ N. Turini,⁴⁴ M. Turner,²⁹ F. Ukegawa,⁵⁴ T. Unverhau,¹⁹ S. Uozumi,⁵⁴ D. Usynin,⁴³ L. Vacavant,²⁸ A. Vaiciulis,⁴⁷ A. Varganov,³³ E. Vataga,⁴⁴ S. Vejcik III,¹⁵ G. Velev,¹⁵ V. Veszpremi,⁴⁶ G. Veramendi,²³ T. Vickey,²³ R. Vidal,¹⁵ I. Vila,¹⁰ R. Vilar,¹⁰ I. Vollrath,³² I. Volobouev,²⁸ M. von der Mey,⁷ P. Wagner,⁵¹ R. G. Wagner,² R. L. Wagner,¹⁵ W. Wagner,²⁵ R. Wallny,⁷ T. Walter,²⁵ T. Yamashita,³⁹ K. Yamamoto,⁴⁰ Z. Wan,⁵⁰ M. J. Wang,¹ S. M. Wang,¹⁶ A. Warburton,³² B. Ward,¹⁹ S. Waschke,¹⁹ D. Waters,³⁰ T. Watts,⁵⁰ M. Weber,²⁸ W. C. Wester III,¹⁵ B. Whitehouse,⁵⁵ A. B. Wicklund,² E. Wicklund,¹⁵ H. H. Williams,⁴³ P. Wilson,¹⁵ B. L. Winer,³⁸ P. Wittich,⁴³ S. Wolbers,¹⁵ M. Wolter,⁵⁵ M. Worcester,⁷ S. Worm,⁵⁰ T. Wright,³³ X. Wu,¹⁸ F. Würthwein,⁸ A. Wyatt,³⁰ A. Yagil,¹⁵ U. K. Yang,¹² W. Yao,²⁸ G. P. Yeh,¹⁵ K. Yi,²⁴ J. Yoh,¹⁵ P. Yoon,⁴⁷ K. Yorita,⁵⁶ T. Yoshida,⁴⁰ I. Yu,²⁷ S. Yu,⁴³ Z. Yu,⁵⁹ J. C. Yun,¹⁵ L. Zanello,⁴⁹ A. Zanetti,⁵³ I. Zaw,²⁰ F. Zetti,⁴⁴ J. Zhou,⁵⁰ A. Zsenei,¹⁸ and S. Zucchelli⁴

(CDF Collaboration)

¹*Institute of Physics, Academia Sinica, Taipei, Taiwan 11529, Republic of China*²*Argonne National Laboratory, Argonne, Illinois 60439, USA*³*Institut de Física d'Altes Energies, Universitat Autònoma de Barcelona, E-08193, Bellaterra (Barcelona), Spain*⁴*Istituto Nazionale di Fisica Nucleare, University of Bologna, I-40127 Bologna, Italy*⁵*Brandeis University, Waltham, Massachusetts 02254, USA*⁶*University of California at Davis, Davis, California 95616, USA*⁷*University of California at Los Angeles, Los Angeles, California 90024, USA*⁸*University of California at San Diego, La Jolla, California 92093, USA*⁹*University of California at Santa Barbara, Santa Barbara, California 93106, USA*¹⁰*Instituto de Física de Cantabria, CSIC-University of Cantabria, 39005 Santander, Spain*¹¹*Carnegie Mellon University, Pittsburgh, Pennsylvania 15213, USA*¹²*Enrico Fermi Institute, University of Chicago, Chicago, Illinois 60637, USA*¹³*Joint Institute for Nuclear Research, RU-141980 Dubna, Russia*¹⁴*Duke University, Durham, North Carolina 27708, USA*¹⁵*Fermi National Accelerator Laboratory, Batavia, Illinois 60510, USA*¹⁶*University of Florida, Gainesville, Florida 32611, USA*¹⁷*Laboratori Nazionali di Frascati, Istituto Nazionale di Fisica Nucleare, I-00044 Frascati, Italy*¹⁸*University of Geneva, CH-1211 Geneva 4, Switzerland*¹⁹*Glasgow University, Glasgow G12 8QQ, United Kingdom*²⁰*Harvard University, Cambridge, Massachusetts 02138, USA*²¹*The Helsinki Group: Helsinki Institute of Physics; and Division of High Energy Physics, Department of Physical Sciences, University of Helsinki, FIN-00044, Helsinki, Finland*²²*Hiroshima University, Higashi-Hiroshima 724, Japan*²³*University of Illinois, Urbana, Illinois 61801, USA*

- ²⁴The Johns Hopkins University, Baltimore, Maryland 21218, USA
²⁵Institut für Experimentelle Kernphysik, Universität Karlsruhe, 76128 Karlsruhe, Germany
²⁶High Energy Accelerator Research Organization (KEK), Tsukuba, Ibaraki 305, Japan
²⁷Center for High Energy Physics: Kyungpook National University, Taegu 702-701; Seoul National University, Seoul 151-742; and Sungkyunkwan University, Suwon 440-746; Korea
²⁸Ernest Orlando Lawrence Berkeley National Laboratory, Berkeley, California 94720, USA
²⁹University of Liverpool, Liverpool L69 7ZE, United Kingdom
³⁰University College London, London WC1E 6BT, United Kingdom
³¹Massachusetts Institute of Technology, Cambridge, Massachusetts 02139, USA
³²Institute of Particle Physics: McGill University, Montréal, Canada H3A 2T8; and University of Toronto, Toronto, Canada M5S 1A7
³³University of Michigan, Ann Arbor, Michigan 48109, USA
³⁴Michigan State University, East Lansing, Michigan 48824, USA
³⁵Institution for Theoretical and Experimental Physics, ITEP, Moscow 117259, Russia
³⁶University of New Mexico, Albuquerque, New Mexico 87131, USA
³⁷Northwestern University, Evanston, Illinois 60208, USA
³⁸The Ohio State University, Columbus, Ohio 43210, USA
³⁹Okayama University, Okayama 700-8530, Japan
⁴⁰Osaka City University, Osaka 588, Japan
⁴¹University of Oxford, Oxford OX1 3RH, United Kingdom
⁴²University of Padova, Istituto Nazionale di Fisica Nucleare, Sezione di Padova-Trento, I-35131 Padova, Italy
⁴³University of Pennsylvania, Philadelphia, Pennsylvania 19104, USA
⁴⁴Istituto Nazionale di Fisica Nucleare, University and Scuola Normale Superiore of Pisa, I-56100 Pisa, Italy
⁴⁵University of Pittsburgh, Pittsburgh, Pennsylvania 15260, USA
⁴⁶Purdue University, West Lafayette, Indiana 47907, USA
⁴⁷University of Rochester, Rochester, New York 14627, USA
⁴⁸The Rockefeller University, New York, New York 10021, USA
⁴⁹Istituto Nazionale di Fisica Nucleare, Sezione di Roma 1, University di Roma “La Sapienza,” I-00185 Roma, Italy
⁵⁰Rutgers University, Piscataway, New Jersey 08855, USA
⁵¹Texas A&M University, College Station, Texas 77843, USA
⁵²Texas Tech University, Lubbock, Texas 79409, USA
⁵³Istituto Nazionale di Fisica Nucleare, University of Trieste, Udine, Italy
⁵⁴University of Tsukuba, Tsukuba, Ibaraki 305, Japan
⁵⁵Tufts University, Medford, Massachusetts 02155, USA
⁵⁶Waseda University, Tokyo 169, Japan
⁵⁷Wayne State University, Detroit, Michigan 48201, USA
⁵⁸University of Wisconsin, Madison, Wisconsin 53706, USA
⁵⁹Yale University, New Haven, Connecticut 06520, USA

(Received 20 October 2004; published 18 February 2005)

We present the results of a search for anomalous production of diphoton events with large missing transverse energy using the Collider Detector at Fermilab. In 202 pb^{-1} of $p\bar{p}$ collisions at $\sqrt{s} = 1.96 \text{ TeV}$ we observe no candidate events, with an expected standard model background of $0.27 \pm 0.07(\text{stat}) \pm 0.10(\text{syst})$ events. The results exclude a lightest chargino of mass less than $167 \text{ GeV}/c^2$, and lightest neutralino of mass less than $93 \text{ GeV}/c^2$ at 95% C.L. in a gauge-mediated supersymmetry-breaking model with a light gravitino.

DOI: 10.1103/PhysRevD.71.031104

PACS numbers: 13.85.Rm, 13.85.Qk, 14.80.-j, 14.80.Ly

The standard model (SM) [1] of elementary particles has been enormously successful, but it is incomplete. For theoretical reasons [2,3], and because of the “ $e\bar{e}\gamma\gamma + \text{missing transverse energy} (\cancel{E}_T)$ ” [4] candidate event recorded by the CDF detector in Run I [5], there is a compelling rationale to search in high-energy collisions for the production of heavy new particles that decay producing the signature of $\gamma\gamma + \cancel{E}_T$. Of particular theoretical interest are supersymmetric (SUSY) models with gauge-mediated SUSY-breaking (GMSB). Characteristically, the effective SUSY-breaking scale (Λ) can be as low as 100 TeV, the lightest SUSY particle is a light gravitino (\tilde{G}) that is assumed to be stable, and the SUSY particles have masses

that may make them accessible at Tevatron energies [2]. In these models the visible signatures are determined by the properties of the next-to-lightest SUSY particle (NLSP) that may be, for example, a slepton or the lightest neutralino ($\tilde{\chi}_1^0$). In the GMSB model investigated here, the NLSP is a $\tilde{\chi}_1^0$ decaying almost exclusively to a photon and a \tilde{G} that penetrates the detector without interacting, producing \cancel{E}_T . SUSY particle production at the Tevatron is predicted to be dominated by pairs of the lightest chargino ($\tilde{\chi}_1^\pm$) and by associated production of a $\tilde{\chi}_1^\pm$ and the next-to-lightest neutralino ($\tilde{\chi}_2^0$). Each gaugino pair cascades down to two $\tilde{\chi}_1^0$'s, leading to a final state of $\gamma\gamma + \cancel{E}_T + X$, where X represents any other final state particles.

In this paper we summarize [6] a search for anomalous production of inclusive $\gamma\gamma + \cancel{E}_T + X$ events in data corresponding to an integrated luminosity of $202 \pm 12 \text{ pb}^{-1}$ [7] of $p\bar{p}$ collisions at $\sqrt{s} = 1.96 \text{ TeV}$ using the CDF II detector [8]. We examine events with two isolated photons with $|\eta| \lesssim 1.0$ and $E_T^\gamma > 13 \text{ GeV}$ for the presence of large \cancel{E}_T . This work extends a previous CDF search [5] for SUSY in this channel by using an upgraded detector, a higher $p\bar{p}$ center-of-mass energy, and a larger data sample. The analysis selection criteria have been reoptimized to maximize, *a priori*, the expected sensitivity to GMSB SUSY based only on the background expectations and the predictions of the model. Similar searches for diphoton + \cancel{E}_T events have been performed elsewhere [9].

We briefly describe the aspects of the CDF II detector relevant to this analysis. The magnetic spectrometer consists of tracking devices inside the 3-m diameter, 5-m long superconducting solenoid magnet operating at 1.4 T. A 90-cm long silicon micro-strip vertex detector, consisting of one single-sided layer and six double-sided layers, with an additional double-sided layer at large η , surrounds the beam pipe. Outside the silicon detector, a 3.1-m long drift chamber with 96 layers of sense wires is used with the silicon detector to determine the momenta of charged particles and the z position of the $p\bar{p}$ interaction (z_{vertex}). The calorimeter, constructed of projective towers, each with an electromagnetic and hadronic compartment, is divided into a central barrel that surrounds the solenoid coil ($|\eta| < 1.1$) and a pair of “end plugs” that cover the region $1.1 < |\eta| < 3.6$. The hadronic compartments of the calorimeter are also used to provide a measurement of the arrival time of the particles depositing energy in each tower. Wire chambers with cathode-strip readout (the CES system), located at shower maximum in the central electromagnetic calorimeter, give two-dimensional profiles of showers. A system of proportional wire chambers in front of the central electromagnetic calorimeters (the CPR system) uses the one-radiation-length-thick magnet coil as a “preradiator” to determine whether showers start before the calorimeter [10]. Muons are identified with a system of planar drift chambers situated outside the calorimeters in the region $|\eta| < 1.0$.

We select candidate events using both online (during data taking) and offline selection requirements. Online, events are selected for the presence of two photon candidates, identified by the three-level trigger as two isolated electromagnetic clusters [10] with $E_T^\gamma > 12 \text{ GeV}$, or two electromagnetic clusters with $E_T^\gamma > 18 \text{ GeV}$ and no isolation requirement. The offline event selection requirements for the diphoton candidate sample are designed to reduce electron and jet/ π^0 backgrounds while accepting well-measured diphoton candidates. We require two central (approximately $0.05 < |\eta| < 1.0$) electromagnetic clusters that: (a) have $E_T^\gamma > 13 \text{ GeV}$; (b) are not near the boundary in ϕ of a calorimeter tower [11]; (c) have the ratio of hadronic to electromagnetic energy, Had/EM , $< 0.055 +$

$0.00045 \cdot E^\gamma (\text{GeV}^{-1})$; (d) have no tracks, or only one track with $p_T < 1 \text{ GeV}/c$, extrapolating to the towers of the cluster; (e) are isolated in the calorimeter and tracking chamber [12]; (f) have a shower shape in the CES consistent with a single photon; (g) have no other significant energy deposited nearby in the CES.

To minimize the number of events with large \cancel{E}_T due to calorimeter energy mismeasurement, we correct for jet (j) energy loss in cracks between detector components and for nonlinear calorimeter response [13]. To avoid any remaining cases where a jet is not fully measured by the calorimeter, we remove events based on the azimuthal opening angle between the \cancel{E}_T direction and the ϕ of any jet with uncorrected $E_T > 10 \text{ GeV}$, $\Delta\phi(\cancel{E}_T, j)$. We require all events to have $10^\circ < \Delta\phi(\cancel{E}_T, j) < 170^\circ$. To reduce beam-related and cosmic-ray backgrounds we require a good vertex with $|z_{\text{vertex}}| < 60 \text{ cm}$ and reject events with significant energy out-of-time with the collision [14]. These backgrounds can also produce \cancel{E}_T equal in magnitude and opposite in direction to a photon, or to the vector sum of the momenta of two photons if they are nearby in ϕ . In this case an event is rejected if there are potential cosmic-ray hits in the muon chamber, within 30 degrees of the photon, that are not matched to any track. Events are also rejected if there is a pattern of energy in the calorimeter indicative of beam-related backgrounds [15]. A sample of 3306 diphoton events pass all candidate selection requirements. The \cancel{E}_T requirement, $\cancel{E}_T > 45 \text{ GeV}$, is determined by the final optimization procedure that is discussed below, after a more complete description of the backgrounds.

Before the \cancel{E}_T requirement, the diphoton candidate sample is dominated by QCD interactions producing combinations of photons and jets faking photons. In each case only small measured \cancel{E}_T is expected, due mostly to energy measurement resolution effects. Standard CDF techniques [10] are used to estimate the individual contributions for the sample to be $47 \pm 6\% \gamma j$, $29 \pm 4\% \gamma\gamma$, and $24 \pm 4\% jj$ production. To estimate the shape of the \cancel{E}_T distribution of this background we use a control sample of similarly produced events that have the same calorimetric response and resolution. We select 7806 events that pass the same photon E_T , z_{vertex} , fiducial, $\Delta\phi(\cancel{E}_T, j)$, beam-related and cosmic-ray background selection requirements, but are allowed to satisfy looser photon identification and isolation requirements [16]. If an event is in the diphoton candidate sample it is rejected from the control sample. The contribution from $e\gamma$ events, discussed below, is also subtracted from the control sample. Since the \cancel{E}_T resolution for a given event is a function of the sum of all the transverse energy in the event (ΣE_T), and we observe a small difference between the ΣE_T distributions of the diphoton candidate and control samples, we correct the \cancel{E}_T in the control sample for this difference [17]. To predict the number of events with large \cancel{E}_T , we normalize the corrected control sample distribution to the number of diphoton candidate events in the region $\cancel{E}_T < 20 \text{ GeV}$, and fit the spectrum

above 10 GeV to a double exponential. We predict $0.01 \pm 0.01(\text{stat}) \pm 0.01(\text{syst})$ events with $\cancel{E}_T > 45$ GeV, where the uncertainty is dominated by differences in the predictions using various control sample selection requirements, the choice of fit function, and the statistical uncertainties of the sample.

Events with an electron and a photon candidate ($W\gamma \rightarrow e\nu\gamma$, $Wj \rightarrow e\nu\gamma_{\text{fake}}$, $Z\gamma \rightarrow ee\gamma$, etc.) can contribute to the diphoton candidate sample when the electron track is lost (by tracking inefficiency or bremsstrahlung) to create a fake photon. For W decays large \cancel{E}_T can come from the neutrinos. This background is estimated using $e\gamma$ events from the data. The diphoton triggers accept electromagnetic clusters with tracks so they provide an efficient and unbiased sample of these events. We find 462 $e\gamma$ events before the \cancel{E}_T requirement. Examining a $Z \rightarrow ee$ sample, we estimate $1.0 \pm 0.4\%$ of electrons will pass the diphoton candidate sample requirements, including charged track rejection. By multiplying the number of observed $e\gamma\cancel{E}_T$ events by the probability that an electron fakes a photon, we estimate $0.14 \pm 0.06(\text{stat}) \pm 0.05(\text{syst})$ background events in the sample with $\cancel{E}_T > 45$ GeV. The uncertainty is dominated by the statistical uncertainty in the fake rate and the uncertainty in the purity of the $e\gamma$ sample.

Beam-related sources and cosmic rays overlapped with a SM event can contribute to the background by producing spurious energy deposits that in turn affect the measured \cancel{E}_T . While the rate at which these events contribute to the diphoton candidate sample is low, most contain large \cancel{E}_T . The spurious clusters can pass photon cuts. The dominant contribution actually comes from sources that produce two photon candidates at once, such as a cosmic muon undergoing bremsstrahlung twice. This background is estimated from the data using a sample of events with no primary collision and two electromagnetic clusters, multiplied by the rate that clusters from cosmic rays pass the diphoton candidate sample requirements. Backgrounds where only one of the photons, or only the \cancel{E}_T , is from a noncollision source, are estimated to be negligible. The total number of events expected from noncollision sources in the $\cancel{E}_T > 45$ GeV sample is $0.12 \pm 0.03(\text{stat}) \pm 0.09(\text{syst})$. The uncertainty includes the uncertainty in the rate that spurious clusters pass the diphoton selection requirements and takes into account the statistics and purity of the sample of events with no primary collision.

The \cancel{E}_T distribution of the diphoton candidate sample (see Fig. 1) shows good agreement with that from the expected backgrounds. Table I summarizes the number of observed events and predicted backgrounds with four different \cancel{E}_T requirements. There are no events with $\cancel{E}_T > 45$ GeV.

Since there is no evidence for events with anomalous \cancel{E}_T in the diphoton candidate sample, we set limits on new particle production from GMSB using the parameters suggested in Ref. [18]. To estimate the acceptance for this scenario we generate GMSB events using ISAJET [19] with

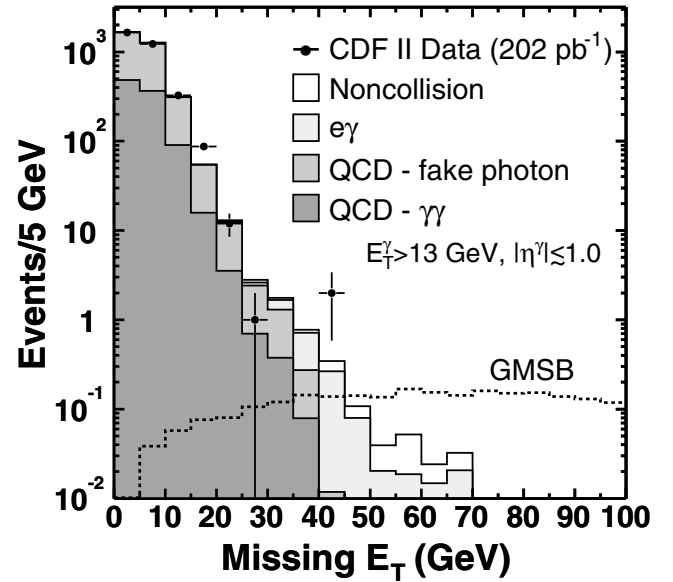


FIG. 1. The \cancel{E}_T spectrum for events with two isolated central photons with $E_T^>13$ GeV and $|\eta| \leq 1.0$ along with the predictions from the GMSB model with a $\tilde{\chi}_1^\pm$ mass of $175 \text{ GeV}/c^2$, normalized to 202 pb^{-1} . The diphoton candidate sample data are in good agreement with the background predictions. There are no events above the $\cancel{E}_T > 45$ GeV threshold. The properties of the two candidates above 40 GeV appear consistent with the expected backgrounds.

CTEQ5L parton distribution functions [20]. The production cross sections from ISAJET are corrected by a K factor of approximately 1.2 to match the next-to-leading order (NLO) prediction [21]. We process the events through the GEANT-based [22] detector simulation, and correct the resulting efficiency with information from data measurements.

Since electrons and photons interact similarly in the calorimeter we investigate the efficiency of the photon identification and isolation selection criteria by using a control sample of electrons from $Z \rightarrow ee$ events. Separate efficiency estimates comparing data and detector simulation agree to within 3%. Using the simulation we estimate that if a photon within the fiducial portion of the detector is isolated, it has an 80% probability of passing the identification and isolation criteria. However, the isolation energy of the photons is predicted from the Monte Carlo to be a strong function of the SUSY scale due to the number and energy of the extra jets produced. We find, for example, the single-photon efficiency to be reduced to 62% at $M_{\tilde{\chi}_1^\pm} = 170 \text{ GeV}/c^2$. This has a significant impact on the sensitivity. We find that the fraction of generated signal events passing all the selection requirements, including $\cancel{E}_T > 45$ GeV, rises linearly from 3.5% at $M_{\tilde{\chi}_1^\pm} = 100 \text{ GeV}/c^2$ to approximately 8% at $180 \text{ GeV}/c^2$. It remains roughly flat for larger masses due to the increasing inefficiency of the $\Delta\phi(\cancel{E}_T, j)$ selection requirement. The relative systematic uncertainty in the efficiency of the photon identification and isolation requirements is ap-

TABLE I. Number of events observed and events expected from background sources as a function of the \cancel{E}_T requirement. Here “QCD” includes the $\gamma\gamma$, γj , and jj processes. The first uncertainty is statistical; the second is systematic.

\cancel{E}_T Requirement	Expected				Observed
	QCD	$e\gamma$	Noncollision	Total	
25 GeV	$4.01 \pm 3.21 \pm 3.76$	$1.40 \pm 0.52 \pm 0.45$	$0.54 \pm 0.06 \pm 0.42$	$5.95 \pm 3.25 \pm 3.81$	3
35 GeV	$0.30 \pm 0.24 \pm 0.22$	$0.84 \pm 0.32 \pm 0.27$	$0.25 \pm 0.04 \pm 0.19$	$1.39 \pm 0.40 \pm 0.40$	2
45 GeV	$0.01 \pm 0.01 \pm 0.01$	$0.14 \pm 0.06 \pm 0.05$	$0.12 \pm 0.03 \pm 0.09$	$0.27 \pm 0.07 \pm 0.10$	0
55 GeV	(negligible)	$0.05 \pm 0.03 \pm 0.02$	$0.07 \pm 0.02 \pm 0.05$	$0.12 \pm 0.04 \pm 0.05$	0

proximately 6.5% per photon. Other significant uncertainties in the Monte Carlo model predictions are from initial/final state radiation (10%), Q^2 of the interaction (3%), and uncertainty in parton distribution functions (5%). Combining these numbers with the 6% luminosity uncertainty gives a total relative systematic uncertainty of 18%.

The kinematic selection requirements defining the final data sample are determined by a study to optimize the expected limit, i.e., without looking at the signal region data. To compute the expected 95% C.L. cross section upper limit we combine the predicted signal and background estimates with the systematic uncertainties using a Bayesian method [23] and follow the prescription described in Ref. [24]. The expected limits are computed as a function of \cancel{E}_T , photon E_T , and $\Delta\phi(\cancel{E}_T, j)$ selection requirements. We find that the best limit is predicted with the selection described above for the diphoton candidate sam-

ple, and $\cancel{E}_T > 45$ GeV. The statistical analysis indicates that the most probable expected result, in the absence of a signal, would be an exclusion of $M_{\tilde{\chi}_1^\pm}$ less than 161 GeV/ c^2 and $M_{\tilde{\chi}_1^0}$ less than 86 GeV/ c^2 .

In the data signal region, with $\cancel{E}_T > 45$ GeV, we observe zero events. Taking into account the 18% systematic uncertainty we set a 95% C.L. upper limit of 3.3 signal events. Figure 2 shows the observed cross section limits as a function of $M_{\tilde{\chi}_1^\pm}$ and $M_{\tilde{\chi}_1^0}$ along with the theoretical LO and NLO production cross sections. Using the NLO predictions we set a limit of $M_{\tilde{\chi}_1^\pm} > 167$ GeV/ c^2 at 95% C.L. From mass relations in the model, we equivalently exclude $M_{\tilde{\chi}_1^0} < 93$ GeV/ c^2 and $\Lambda < 69$ TeV.

In conclusion, we have searched 202 pb $^{-1}$ of inclusive diphoton events at CDF run II for anomalous production of missing transverse energy as evidence of new physics. We find good agreement with standard model expectations. We find no events above the *a priori* \cancel{E}_T threshold, and thus observe no new $ee\gamma\gamma\cancel{E}_T$ candidates. Using these results, we have set limits on the lightest chargino $M_{\tilde{\chi}_1^\pm} > 167$ GeV/ c^2 and $M_{\tilde{\chi}_1^0} > 93$ GeV/ c^2 at 95% C.L. in a GMSB model. This limits are an improvement over previous CDF and D0 limits and are comparable to LEP II for similar models [9].

We thank the Fermilab staff and the technical staffs of the participating institutions for their vital contributions. This work was supported by the U.S. Department of Energy and National Science Foundation; the Italian Istituto Nazionale di Fisica Nucleare; the Ministry of Education, Culture, Sports, Science and Technology of Japan; the Natural Sciences and Engineering Research Council of Canada; the National Science Council of the Republic of China; the Swiss National Science Foundation; the A.P. Sloan Foundation; the Bundesministerium fuer Bildung und Forschung, Germany; the Korean Science and Engineering Foundation and the Korean Research Foundation; the Particle Physics and Astronomy Research Council and the Royal Society, United Kingdom; the Russian Foundation for Basic Research; the Comision Interministerial de Ciencia y Tecnologia, Spain; and in part by the European Community’s Human Potential Programme under Contract No. HPRN-CT-2002-00292, Probe for New Physics.

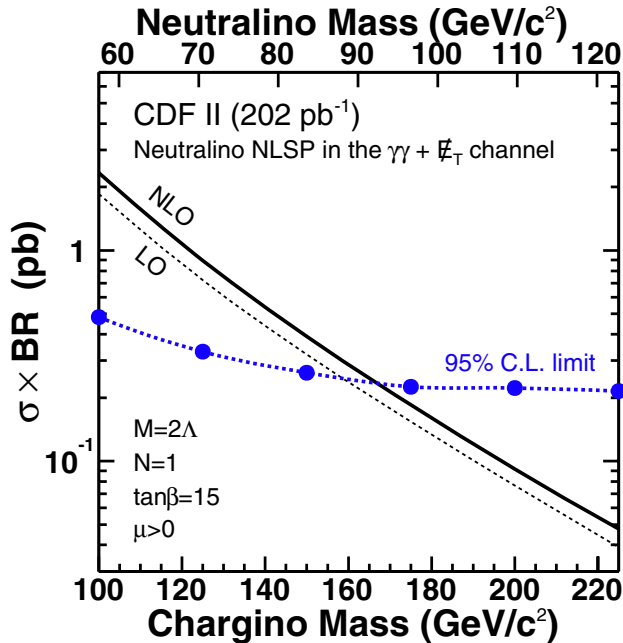


FIG. 2 (color online). The 95% C.L. upper limits on the total production cross section times branching ratio versus $M_{\tilde{\chi}_1^\pm}$ and $M_{\tilde{\chi}_1^0}$ for the light gravitino scenario using the parameters proposed in [18]. The lines show the experimental limit and the LO and NLO theoretically predicted cross sections. We set limits of $M_{\tilde{\chi}_1^\pm} > 167$ GeV/ c^2 and $M_{\tilde{\chi}_1^0} > 93$ GeV/ c^2 at 95% C.L.

- [1] See, for example, F. Halzen and A. D. Martin, *Quarks and Leptons* (John Wiley & Sons, New York, 1984); C. Quigg, *Gauge Theories of the Strong, Weak, and Electromagnetic Interactions* (Addison-Wesley, Reading, MA, 1983); I. S. Hughes, *Elementary Particles* (Cambridge University Press, Cambridge, England, 1990).
- [2] S. Dimopoulos, S. Thomas, and J. D. Wells, Nucl. Phys. **B488**, 39 (1997); S. Ambrosanio, G. D. Kribs, and S. P. Martin, Phys. Rev. D **56**, 1761 (1997); G. F. Giudice and R. Rattazzi, Phys. Rep. **322**, 419 (1999); S. Ambrosanio, G. Kane, G. Kribs, S. Martin, and S. Mrenna, Phys. Rev. D **55**, 1372 (1997).
- [3] R. Culbertson *et al.*, hep-ph/0008070.
- [4] We use a cylindrical coordinate system that defines z as the longitudinal axis and along the proton beam axis, in which θ is the polar angle, ϕ is the azimuthal angle, and $\eta = -\ln[\tan(\theta/2)]$. In general, all quantities are defined from $z_{\text{vertex}} = 0$, $E_T = E \sin\theta$, and $p_T = p \sin\theta$ where E is the energy measured by the calorimeter and \underline{p} the momentum measured in the tracking system. $\cancel{E}_T = -\sum_i E_T^i \vec{n}_i$ where \vec{n}_i is a unit vector that points from the interaction vertex to the i th calorimeter tower in the transverse plane. $|\cancel{E}_T|$ is the magnitude of \cancel{E}_T .
- [5] CDF Collaboration, F. Abe *et al.*, Phys. Rev. Lett. **81**, 1791 (1998); Phys. Rev. D **59**, 092002 (1999).
- [6] M. S. Kim, Fermilab Report No. FERMILAB-THESIS-2004-41 (unpublished).
- [7] S. Klimenko *et al.*, Fermilab Report No. FERMILAB-FN-0741, 2003; D. Acosta *et al.*, Nucl. Instrum. Methods Phys. Res., Sect. A **494**, 57 (2002).
- [8] CDF II Collaboration, R. Blair *et al.*, Fermilab Report No. FERMILAB-PUB-96/390-E, 1996.
- [9] D0 Collaboration, S. Abachi *et al.*, Phys. Rev. Lett. **78**, 2070 (1997); B. Abbott *et al.*, Phys. Rev. Lett. **80**, 442 (1998); V. Abazov *et al.*, Phys. Rev. Lett. **94**, 041801 (2005); ALEPH Collaboration, A. Heister *et al.*, Eur. Phys. J. C **25**, 339 (2002); L3 Collaboration, M. Acciarri *et al.*, Phys. Lett. B **472**, 420 (2000); OPAL Collaboration, G. Abbiendi *et al.*, Eur. Phys. J. C **18**, 253 (2000); DELPHI Collaboration, P. Abreu *et al.*, Eur. Phys. J. C **17**, 53 (2000).
- [10] CDF Collaboration, F. Abe *et al.*, Phys. Rev. D **52**, 4784 (1995); D. Acosta *et al.*, Phys. Rev. D **65**, 112003 (2002).
- [11] The fiducial region has $\sim 87\%$ coverage in the central region.
- [12] To reject hadronic backgrounds that fake prompt photons, candidates are required to be isolated in the calorimeter and tracking chamber. In the calorimeter the isolation is defined as the energy in a cone of 0.4 in $\eta - \phi$ space, minus the photon cluster energy, and corrected for energy loss into cracks as well as the number of reconstructed $p\bar{p}$ interactions in the event. We require isolation $< 0.1 \times E_T^\gamma$ for $E_T^\gamma < 20$ GeV, and < 2.0 GeV + $0.02 \times (E_T^\gamma - 20$ GeV) for $E_T^\gamma > 20$ GeV. In the tracking chamber we require the scalar sum of the p_T of all tracks in a cone of 0.4 to be < 2.0 GeV + $0.005 \times E_T^\gamma$, where all values of E_T^γ are in GeV.
- [13] See F. Abe *et al.*, Phys. Rev. D **45**, 1448 (1992) for a description of the jet-finding algorithm and the jet energy corrections. Jets are reconstructed with a cone in $\eta - \phi$ space of radius 0.4.
- [14] We require the time of arrival of the energy in all hadron calorimeter towers with at least 0.5 GeV to be within 3σ of the expected value.
- [15] M. Karagöz Ünel and R. Tesarek, Nucl. Instrum. Methods Phys. Res., Sect. A **506**, 7 (2003).
- [16] The identification and isolation requirements for the control sample are: (a) isolation $< 0.15 \times E_T^\gamma$ for $E_T^\gamma < 20$ GeV, and < 3.0 GeV + $0.02 \times (E_T^\gamma - 20$ GeV) for $E_T^\gamma > 20$ GeV; (b) tracking isolation < 5 GeV/ c ; (c) Had/EM < 0.125 ; (d) at most one track, and no tracks with $p_T > 0.25E_T/c$.
- [17] The means of the ΣE_T distributions (where ΣE_T excludes the photon E_T 's) are separated by approximately 6%. This is most likely due to different fractional contributions from $\gamma\gamma$, γj , and jj processes. The corrections are made by taking the expected shape of the \cancel{E}_T distribution from the control sample as a function of ΣE_T , and normalizing to the observed ΣE_T distribution in the signal sample.
- [18] B. C. Allanach *et al.*, Eur. Phys. J. C **25**, 113 (2002). We take the messenger mass scale $M_M = 2\Lambda$, $\tan(\beta) = 15$, $\text{sign}(\mu) = 1$, the number of messenger fields $N_M = 1$, and negligibly short $\tilde{\chi}_1^0$ lifetimes.
- [19] H. Baer, F. E. Paige, S. D. Protopopescu, and X. Tata, hep-ph/0001086.
- [20] H. L. Lai *et al.*, Eur. Phys. J. C **12**, 375 (2000).
- [21] The K factor has a small dependence on the $\tilde{\chi}_1^\pm$ mass and is taken from W. Beenakker *et al.*, Phys. Rev. Lett. **83**, 3780 (1999); and T. Plehn, <http://pheno.physics.wisc.edu/~plehn/prospino/prospino.html>.
- [22] R. Brun *et al.*, CERN Report No. CERN-DD/EE/84-1, 1987.
- [23] J. Conway, CERN Yellow Book Report No. CERN 2000-005, 2000, p. 247. We assume a flat prior in the production cross section up to a high cutoff; the limit is not significantly dependent on the value of the cutoff.
- [24] E. Boos, A. Vologdin, D. Toback, and J. Gaspard, Phys. Rev. D **66**, 013011 (2002).